(12) UK Patent Application (19) GB (11) 2 298 735 (13) A

(43) Date of A Publication 11.09.1996

(21) Application No 9504666.0

(22) Date of Filing 08.03.1995

(71) Applicant(s)
Sharp Kabushiki Kaisha

(Incorporated in Japan)

22-22, Nagaike-cho, Abeno-ku, Osaka 545, Japan

(72) Inventor(s)
Geoffrey Duggan
Judy Megan Rorison
Nobuaki Teraguchi
Yoshitaka Tomomura

(74) Agent and/or Address for Service
Marks & Clerk
Alpha Tower, Suffolk Street Queensway,
BIRMINGHAM, B1 1TT, United Kingdom

(51) INT CL^6
H01S 3/025 , G02F 1/015 , H01L 31/0352 33/00

(52) UK CL (Edition O)
H1K KKAS K1EA K1EA1 K1EB K1FX K2R3A K2R3E K2S1C K2S1D K2S1E K2S16 K2S19 K2S2D K2S2P K2S21 K2S27 K2S3D K2S4B K9E K9M1 K9N2 K9N3 K9P3 K9S

(56) Documents Cited
EP 0614253 A1 **EP 0334759 A2** **WO 94/00884 A1**
WO 92/08250 A **US 5324959 A** **US 4866488 A**
US 4620206 A

(58) Field of Search
UK CL (Edition N) **H1K KKAS**
INT CL^6 **G02F , H01L , H01S**
Online : WPI, INSPEC

(54) Semiconductor device having a miniband

(57) A semiconductor device (eg laser, modulator, detector) is provided in which carrier transport towards the active region thereof is enhanced by the formation of a miniband (18) within a superlattice region of the device having a repeating pattern of first (10) and second (12) semiconductor regions. The pattern repeat period is typically less than 25 angstroms. The superlattice may comprise MgS/ZnSe, MgSSe/ZnSSe II-VI semiconductors, alternatively the superlattice may be based on the AlGaIn N or AlGaIn P III-V semiconductor alloy systems.

GB 2 298 735 A

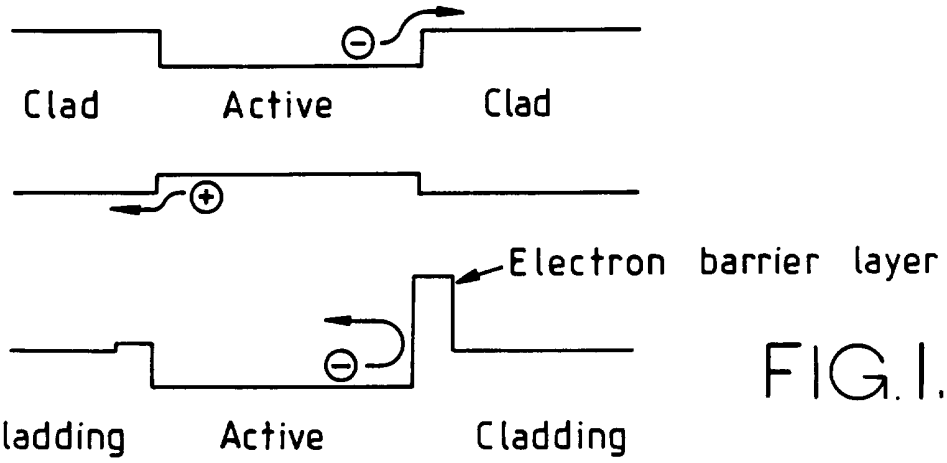

FIG.1.

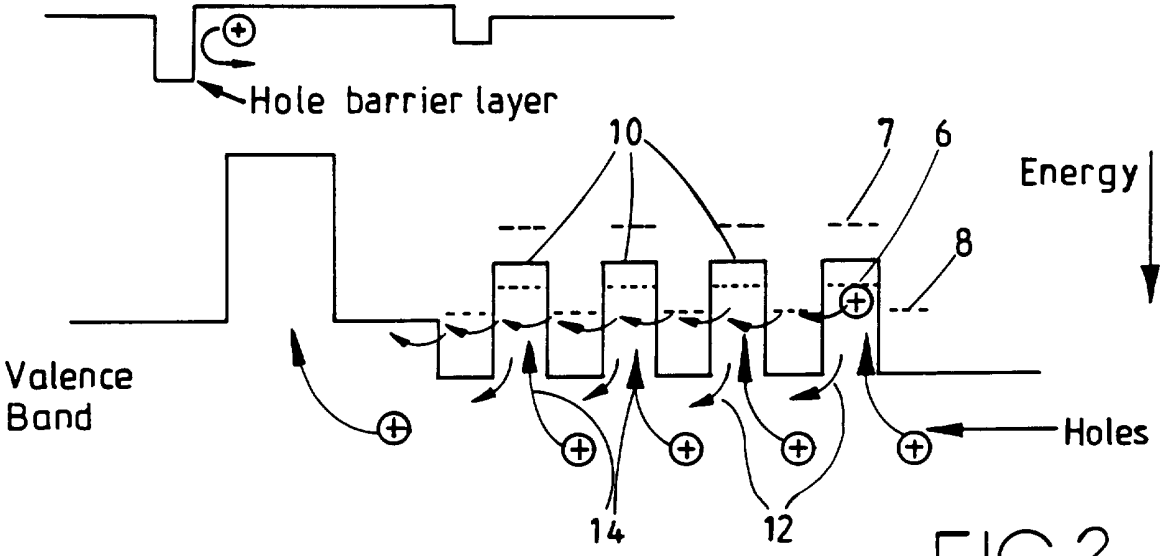

FIG.2.

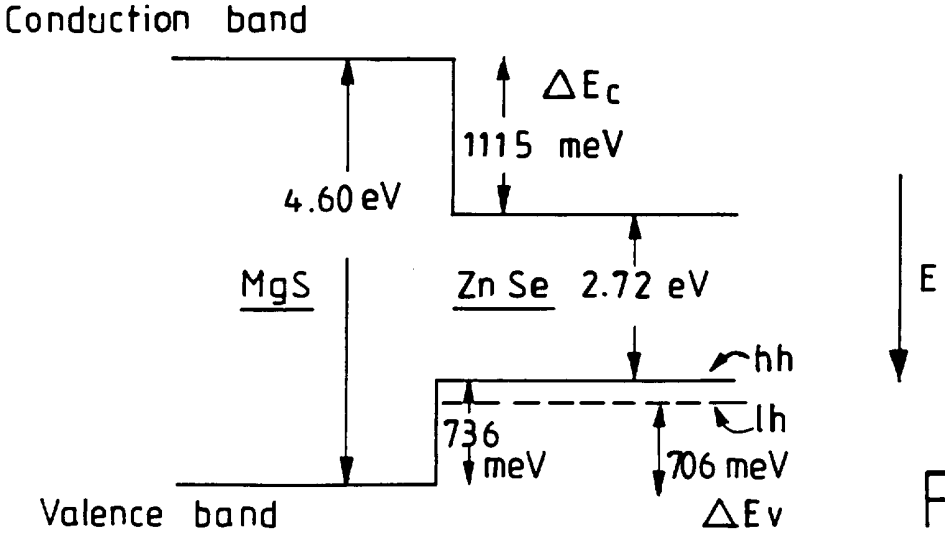

FIG.3.

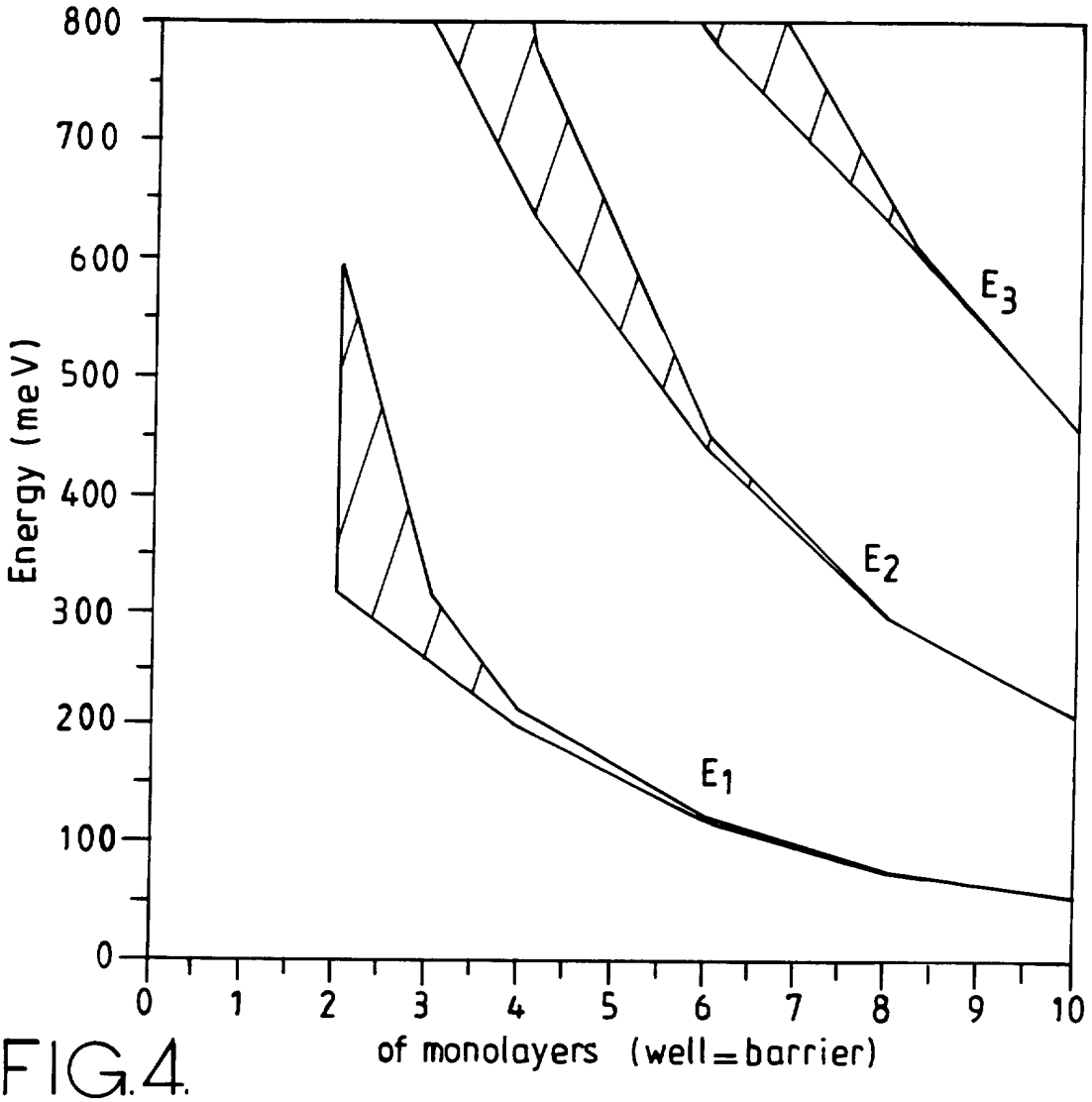
800
700
600
500
400
300
200
100
0
Energy (meV)
0
1
2
3
4
5
6
7
8
9
10
of monolayers (well=barrier)
E3
E2
E1

FIG.4.

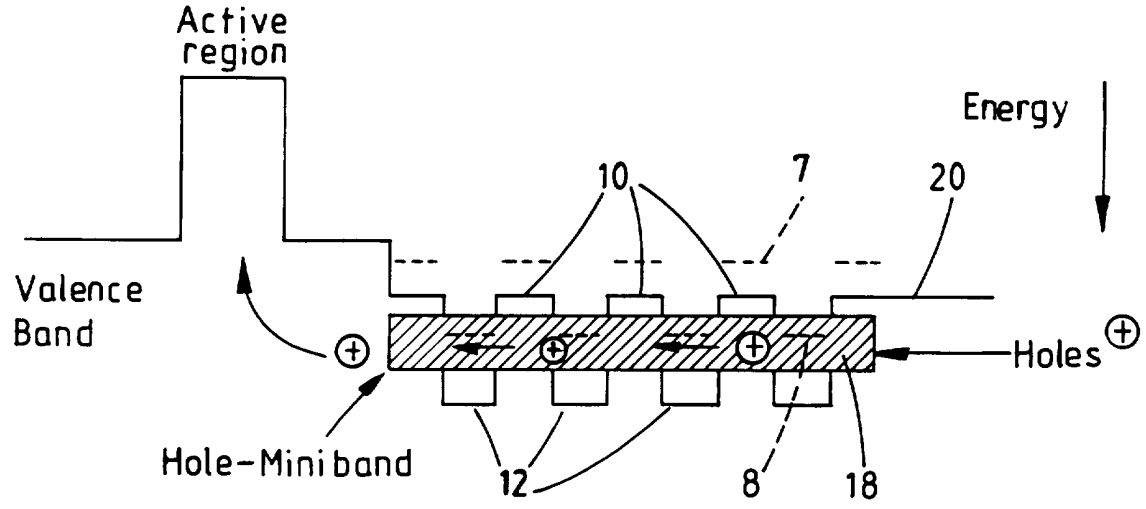
Active region
Energy
10
7
20
Valence Band
Holes
Hole-Miniband
12
8
18

FIG.6.

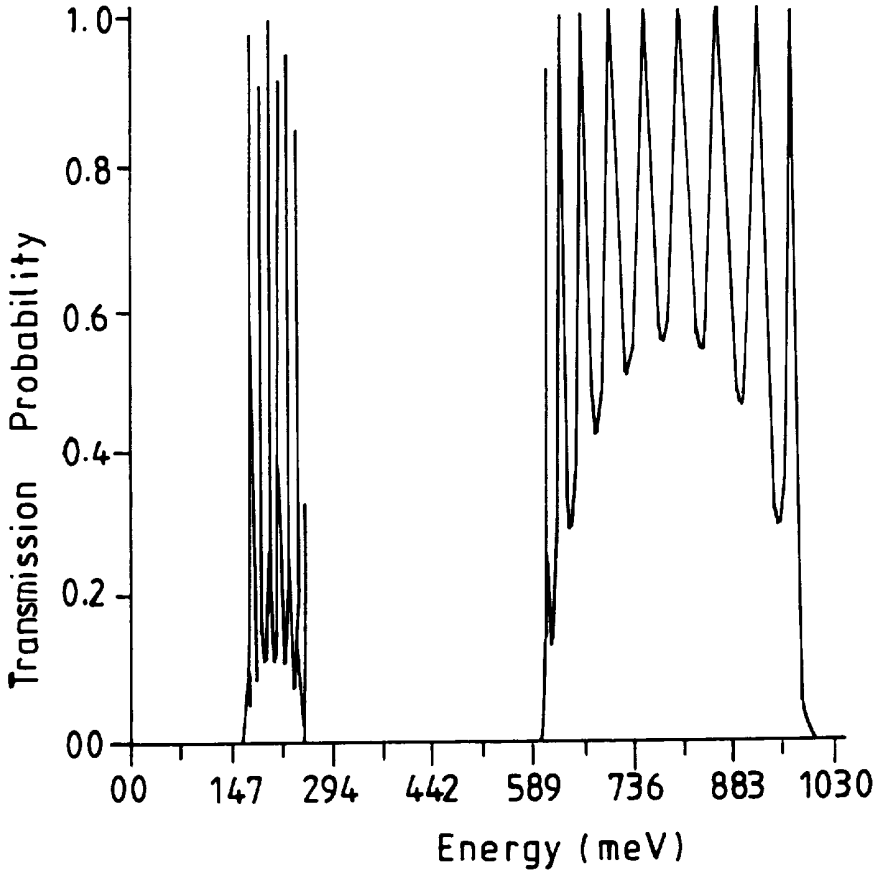
1.0
0.8
0.6
0.4
0.2
00
Transmission Probability
00
147
294
442
589
736
883
1030
Energy (meV)

FIG.5.

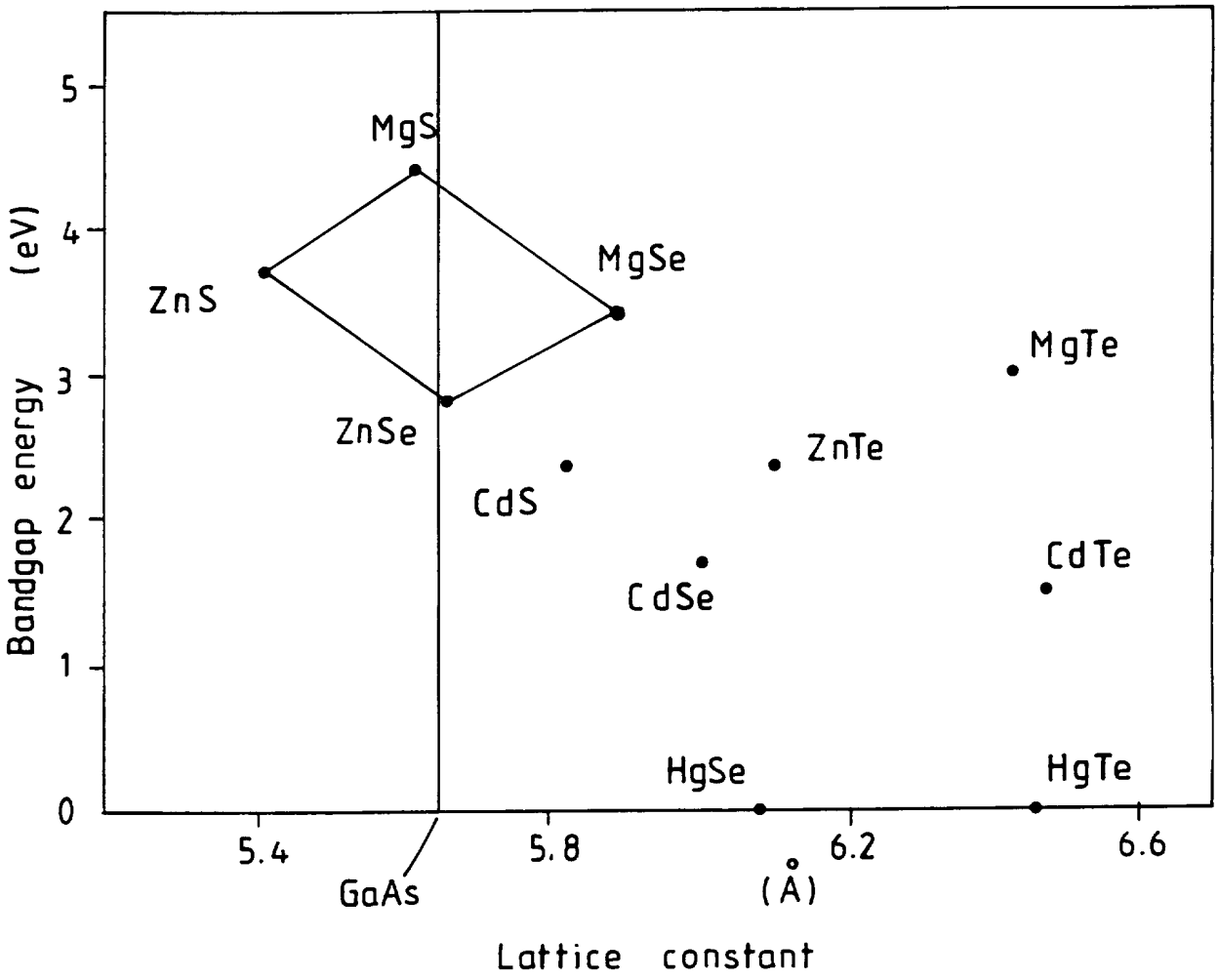
Bandgap energy (eV)
5
4
3
2
1
0
MgS
MgSe
ZnS
ZnSe
MgTe
ZnTe
CdS
CdTe
CdSe
HgSe
HgTe
5.4
5.8
6.2
6.6
GaAs
(Å)
Lattice constant

FIG.7.

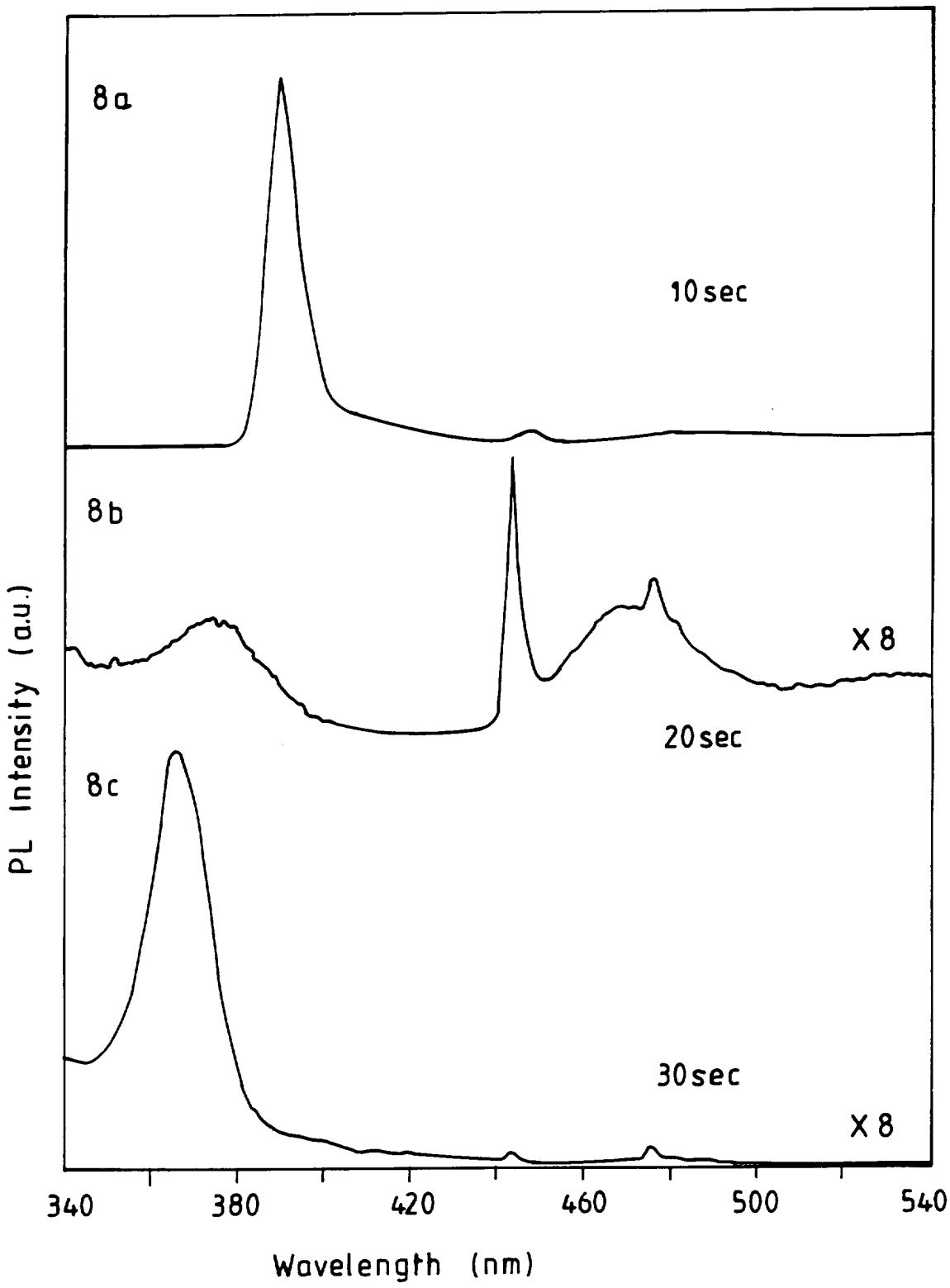
8a
10sec
8b
X 8
20sec
8c
30sec
X 8
PL Intensity (a.u.)
340
380
420
460
500
540
Wavelength (nm)

FIG.8.

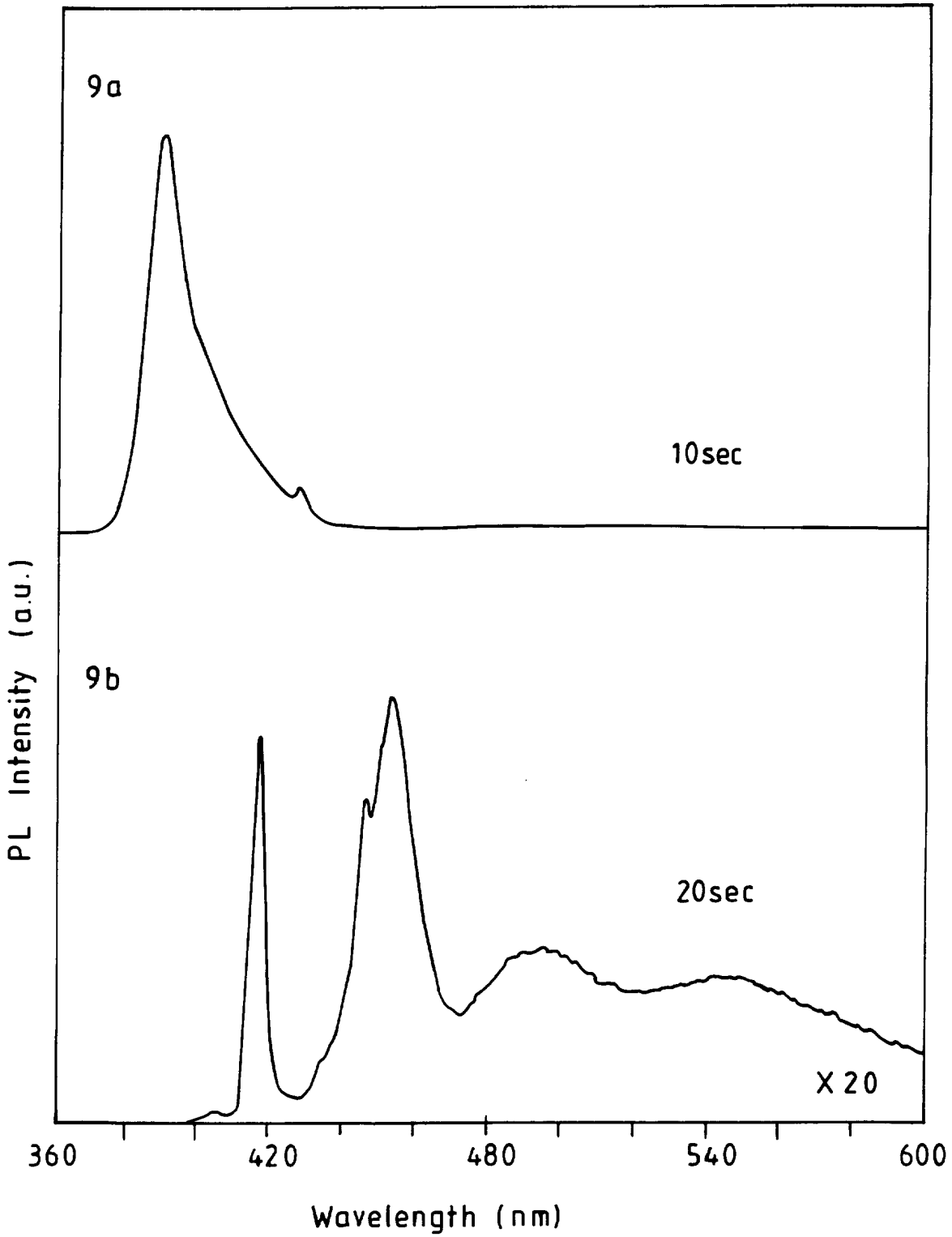
9a
10sec
9b
20sec
X 20
PL Intensity (a.u.)
360
420
480
540
600
Wavelength (nm)

FIG.9.

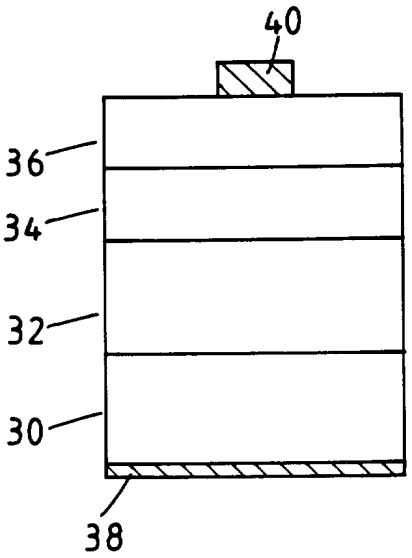

(a) n-i-n

FIG.10.

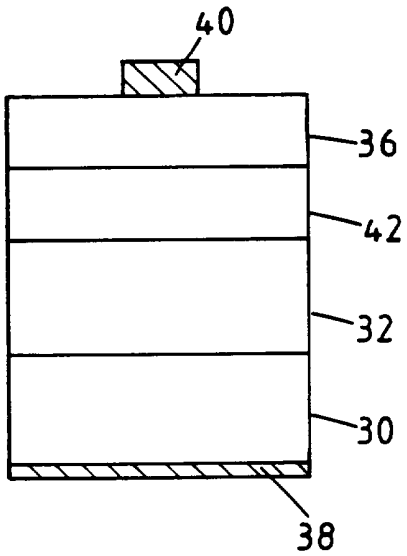

(b) n-n-n

FIG.11.

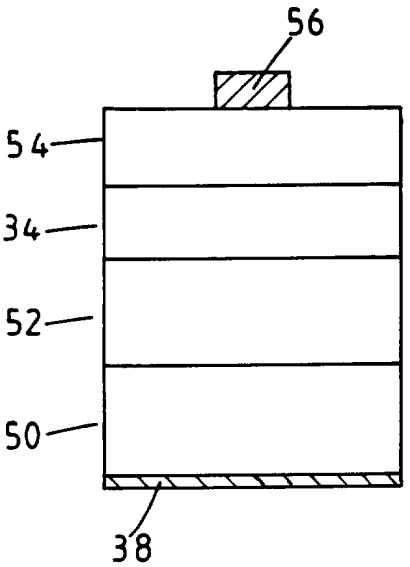

(a) p-i-p

FIG.14.

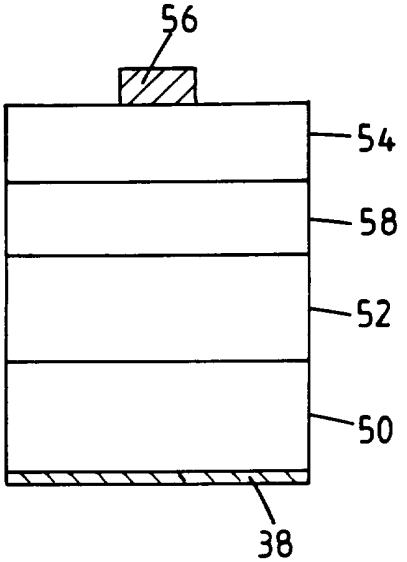

(b) p-p-p

FIG.15.

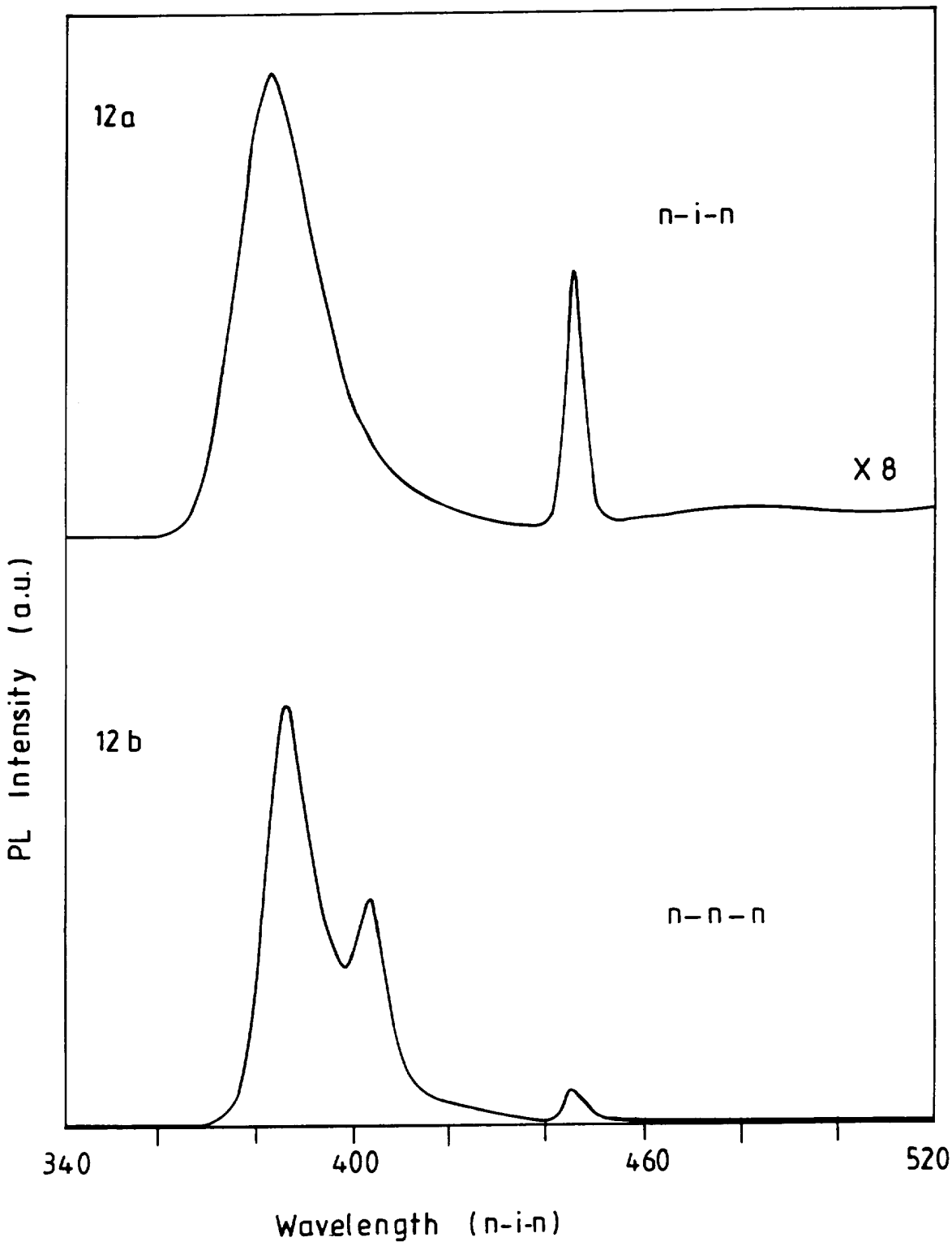
12a
n-i-n
X 8
12 b
n-n-n
PL Intensity (a.u.)
340
400
460
520
Wavelength (n-i-n)

FIG.12.

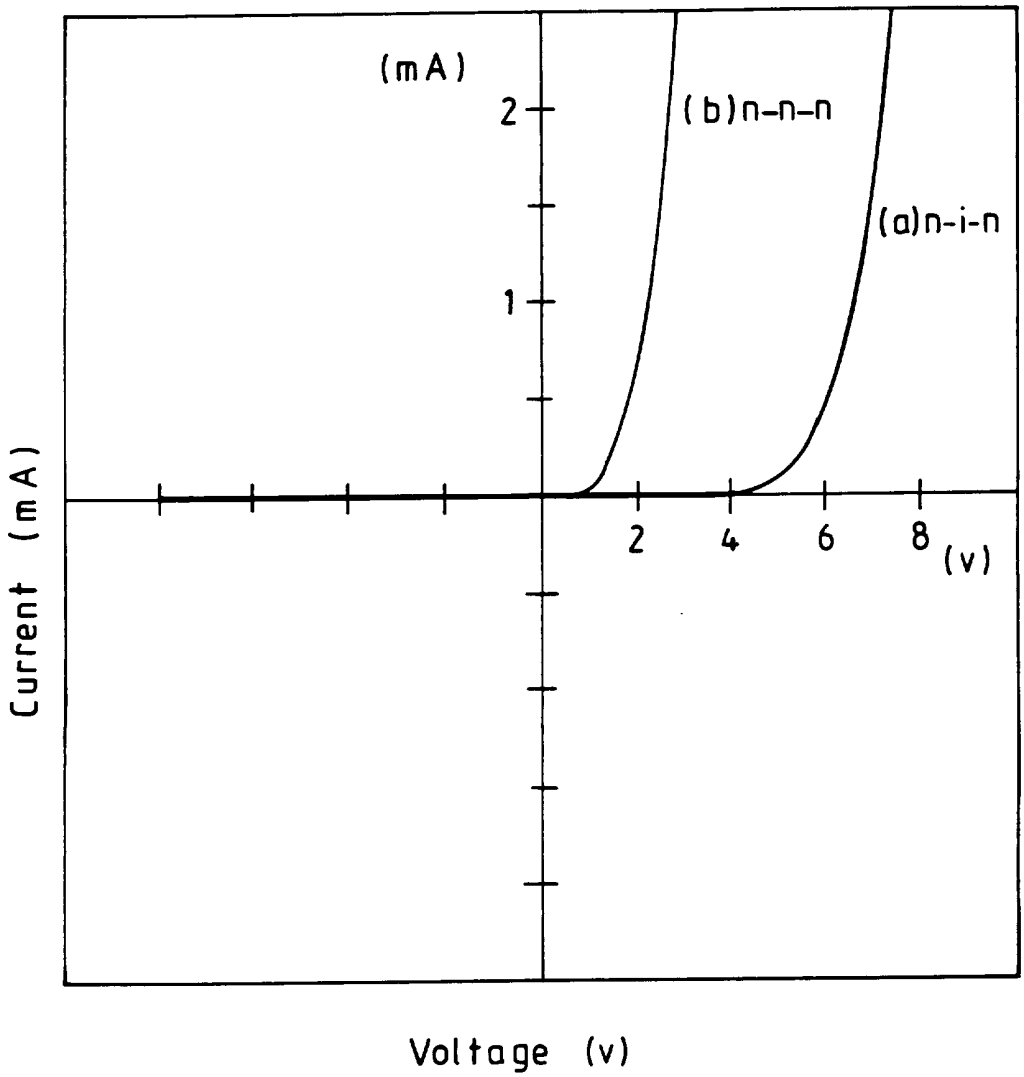

FIG.13.

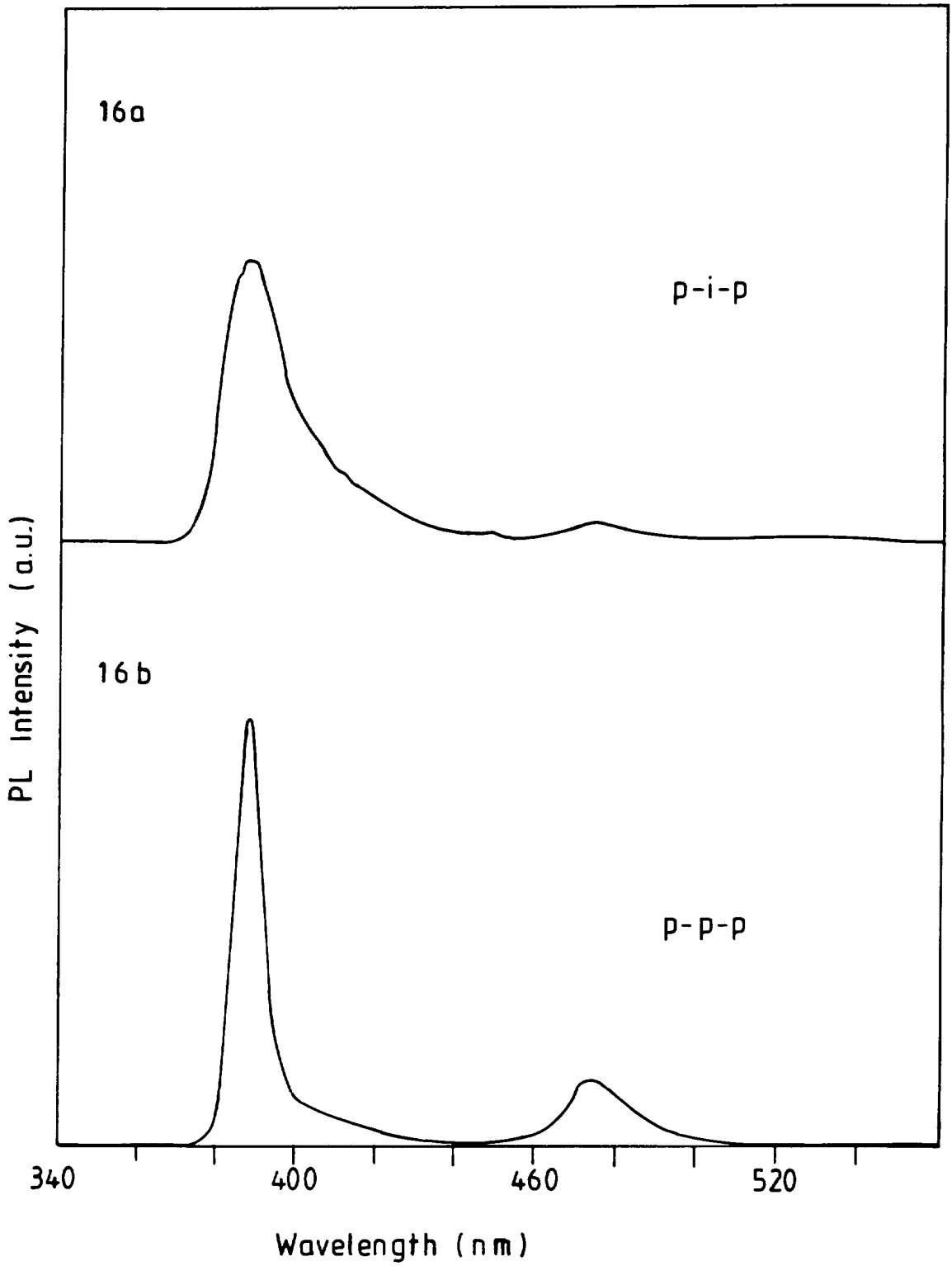

FIG.16.

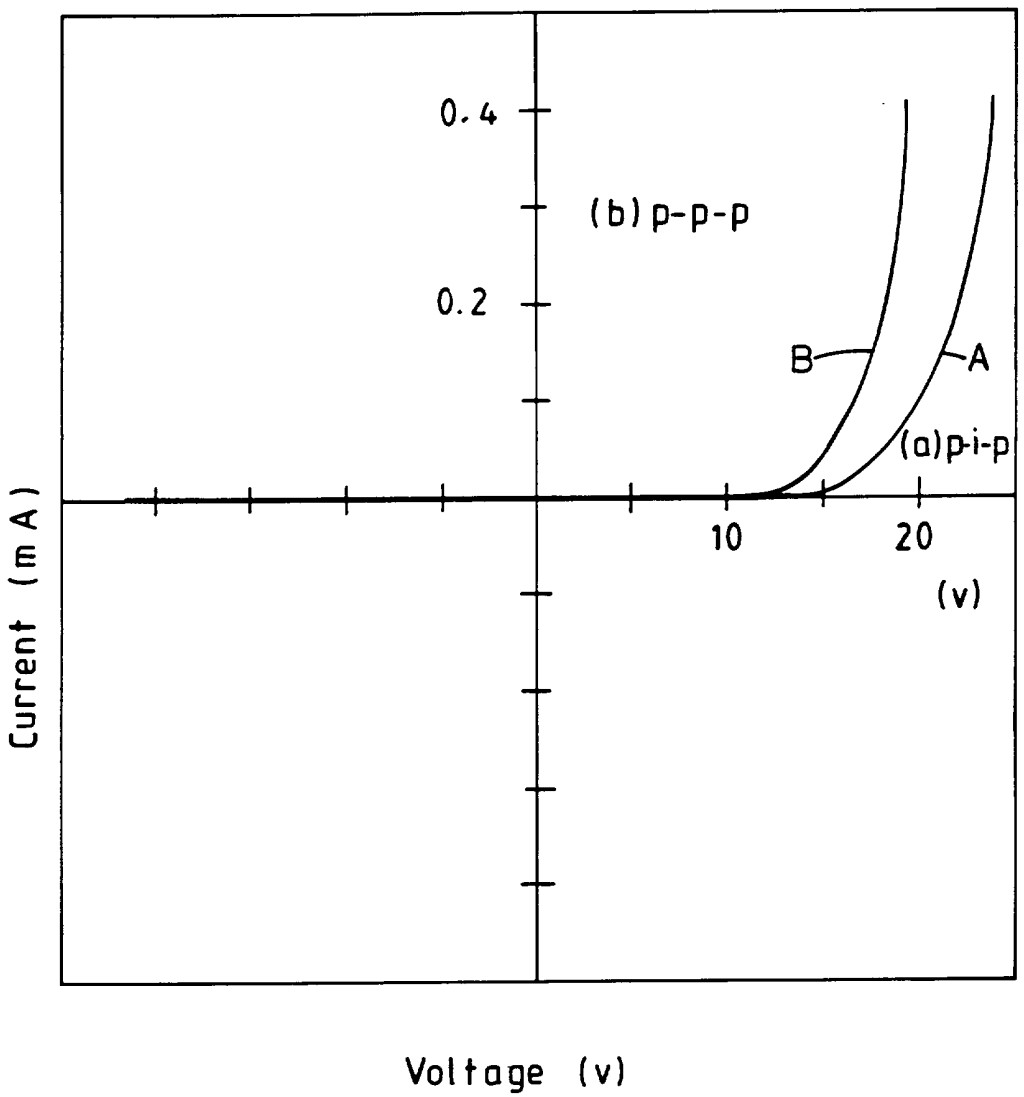

FIG.17.

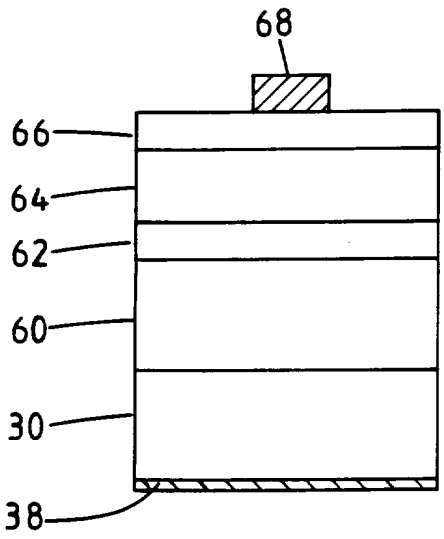

FIG.18.

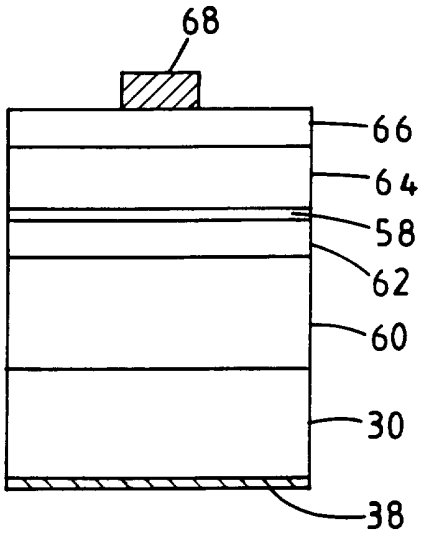

FIG.19.

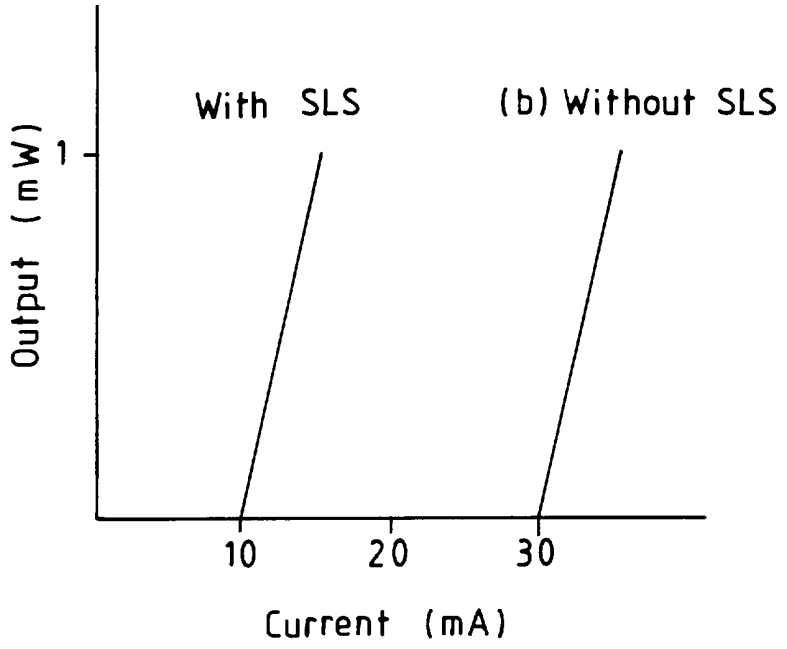

FIG.20.

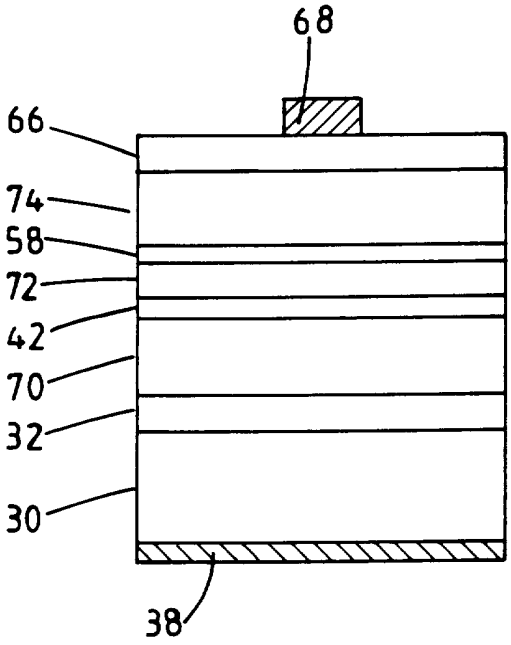

FIG.21.

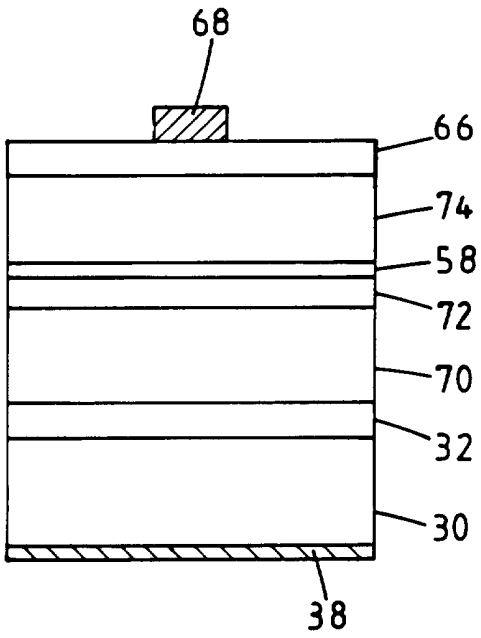

FIG.22.

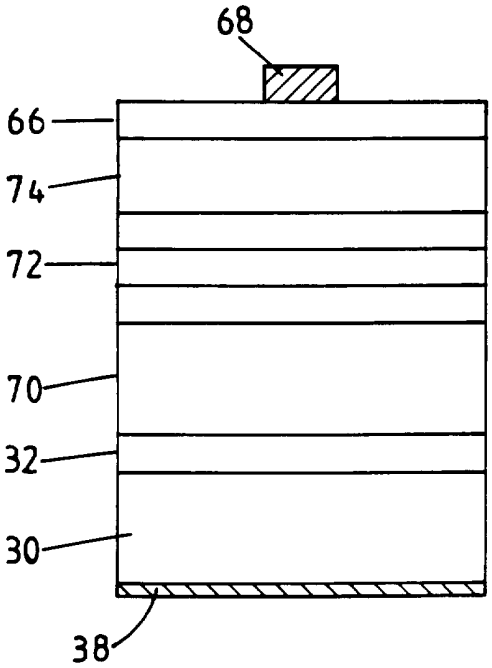

FIG.23.

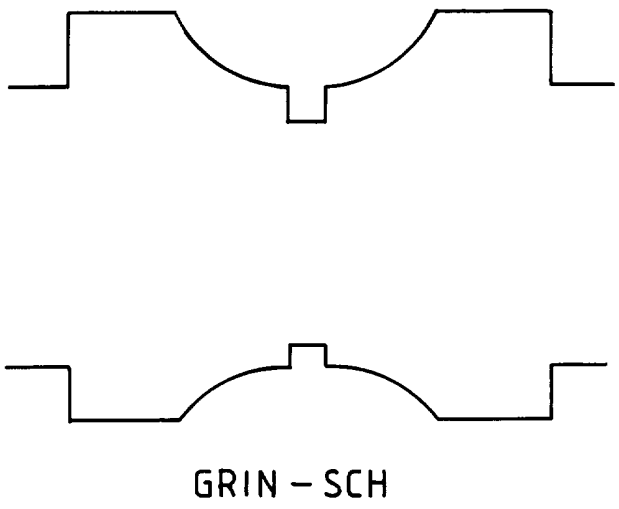

FIG.24.

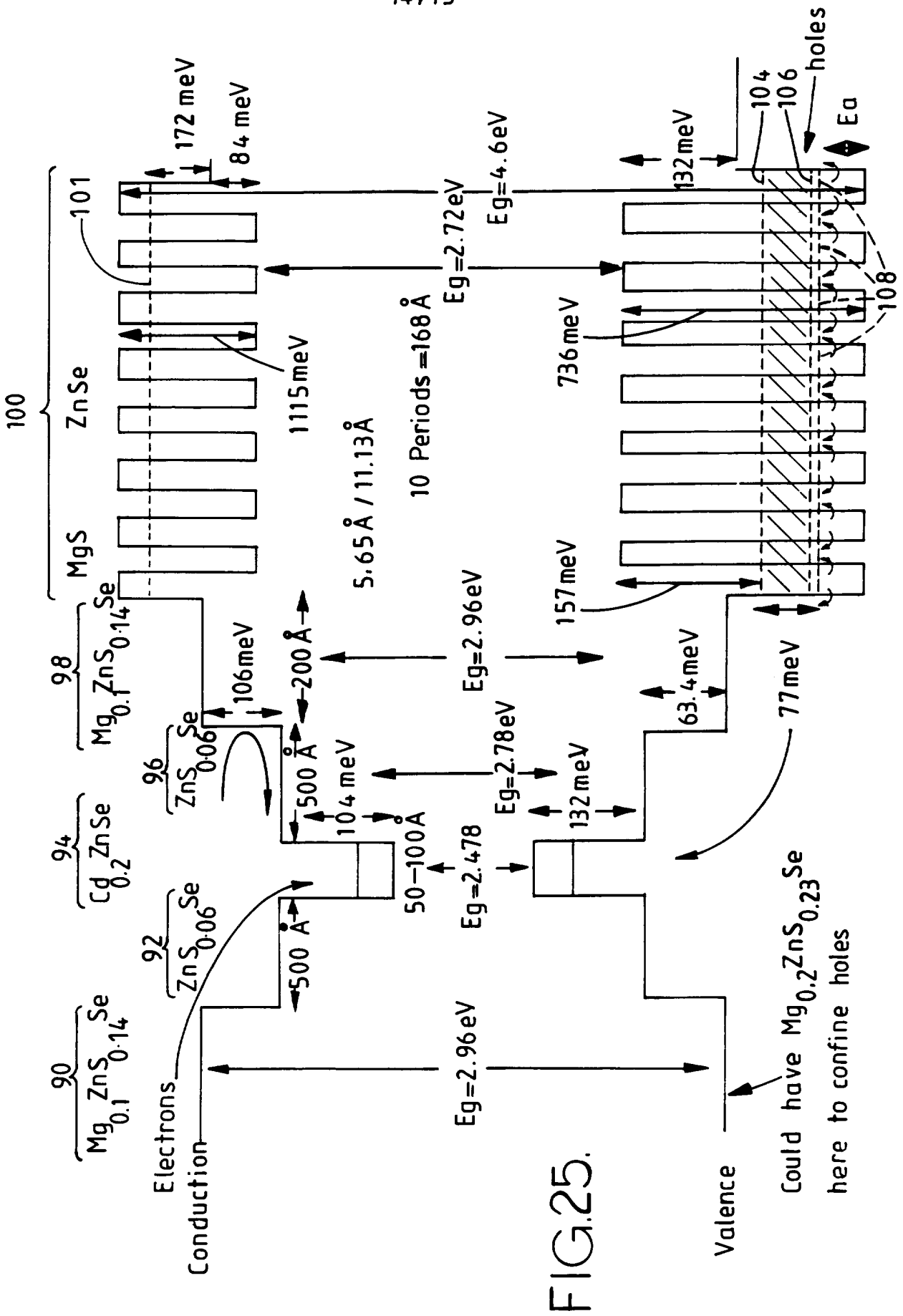
100
ZnSe
MgS
101
172 meV
84 meV
1115meV
10 Periods =168 Å
5.65 Å / 11.13 Å
Eg=2.72eV
Eg=4.6eV
132meV
104
106
holes
Ea
108
736meV
157meV
98
$Mg_{0.1}ZnS_{0.14}Se$
106meV
200 Å
Eg=2.96eV
63.4meV
77meV
96
$ZnS_{0.06}Se$
500 Å
104 meV
Eg=2.78eV
132meV
94
$Cd_{0.2}ZnSe$
50–100Å
Eg=2.478
92
$ZnS_{0.06}Se$
500 Å
90
$Mg_{0.1}ZnS_{0.14}Se$
Electrons
Conduction
Eg=2.96eV
Valence
Could have $Mg_{0.2}ZnS_{0.23}Se$
here to confine holes

FIG.25.

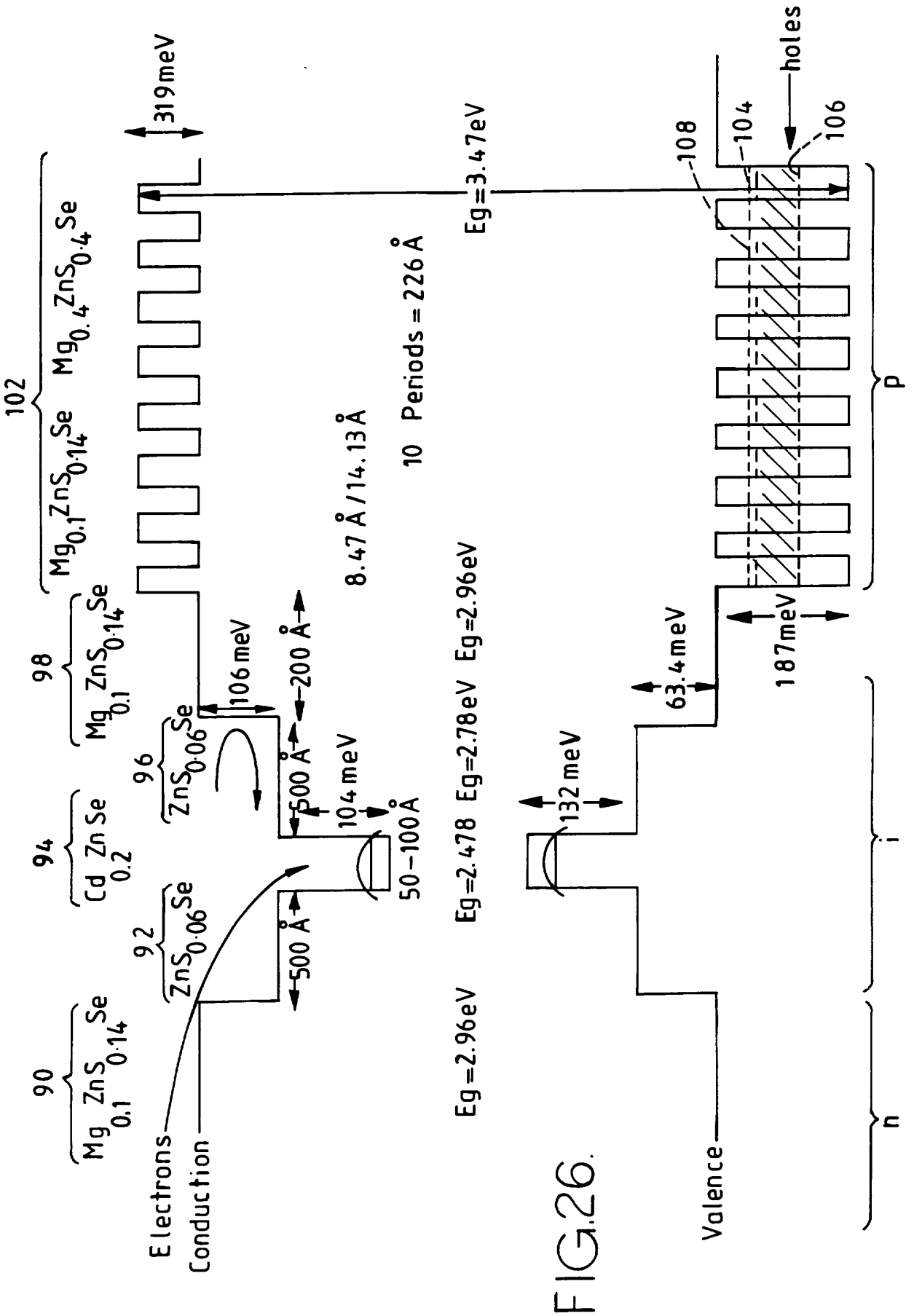
102
$Mg_{0.1}ZnS_{0.14}Se$
$Mg_{0.4}ZnS_{0.4}Se$
319meV
Eg=3.47eV
108
104
holes
106
p
98
$Mg_{0.1}ZnS_{0.14}Se$
106 meV
200 Å
96
$ZnS_{0.06}Se$
500 Å
104 meV
50–100Å
8.47 Å / 14.13 Å
10 Periods = 226 Å
94
Cd Zn Se
0.2
92
$ZnS_{0.06}Se$
500 Å
90
$Mg_{0.1}ZnS_{0.14}Se$
Electrons
Conduction
Eg=2.96eV
Eg=2.478
Eg=2.78eV
Eg=2.96eV
132 meV
63.4meV
187meV
i
n
Valence

FIG.26.

SEMICONDUCTOR DEVICE HAVING A MINIBAND

The present invention relates to a semiconductor device having a miniband. Such a miniband improves the transportation of charges within the semiconductor device. In particular the miniband improves the operation of semiconductor light sources, modulators and detectors operating in the green or blue regions of the electromagnetic spectrum.

Researchers in the field of semiconductor optical devices have been investigating ways to provide light sources operating in the blue-green optical region. The properties of II-VI compound semiconductors as guide and cladding materials have been reported.

Initial research on blue-green optical devices reported the use of ZnSe and $ZnS_{0.07}Se_{0.93}$ as guide and cladding layer materials, respectively ("Blue-green laser diodes", M. A. Haase et al., Appl. Phys. Lett. 59 p.1272). Some researchers reported that a $ZnS_{0.07}Se_{0.93}$ guide layer and a ZnMgSSe cladding layer lattice matched to GaAs were necessary for the reduction of threshold current and shortening the lasing wavelength ("Room temperature continuous operation of blue-green laser diode", N. Nakayama et al., Electron. Lett. 29 P.1488).

However, the rapid decrease of net acceptor concentration (Na-Nd) with increasing bandgap energy in ZnMgSSe, which was believed to be a good material for the reduction of threshold current and shortening the lasing wavelength, may define limits of the threshold current and the lasing wavelength. The shortest lasing wavelength that the applicants are aware of is 489.9nm and the threshold current density is 1.5kA/cm^3 for continuous operation at room temperature. ("Continuous-wave operation

of 489.9nm blue laser diode at room temperature", N. Nakayama et al., Electron. Lett. 29 p.2164).

In order to avoid the drastic reduction of net acceptor concentration (Na-Nd) and to improve doping efficiency, the use of a modulation doping technique has been proposed ("Doping in a superlattice structure: improved hole activation in wide-gap II-VI materials", I. Suemune, J. Appl. Phys. 67 p.2364). Furthermore, another technique of introducing a superlattice structure has also been proposed ("One-hour-long room temperature CW operation of ZnMgSSe-based blue-green laser diodes", A. Ishibashi et al., 7th annual meeting on the IEEE Lasers and Electro-Optics Society (1994)).

Researchers have found it difficult to obtain blue colour laser diodes with the wavelength shorter than 480 nm with continuous wave operation at room temperature even when using a ZnMgSSe cladding layer lattice matched to GaAs.

In order to reduce the threshold current of a semiconductor laser and improve its temperature characteristics, it is necessary to increase the band discontinuity between active layer 2 and cladding layer 4 shown schematically in Figure 1. This reduces an overflow of carriers from active layer 2 to cladding layer 4 which results in the effective carrier confinement inside active layer. Using carrier barrier layers depicted in Figure 1, carriers can be confined effectively which results in the reduction of threshold current.

To shorten the lasing wavelength, it is necessary to increase the bandgap energy of active layer 2. The bandgap energy of cladding layer 4 should

also be increased. Otherwise, the band discontinuity between the active and cladding layers will be reduced and will result in the increase of carrier overflow and consequential increase of threshold current. Therefore, it is necessary to increase the bandgap energy of the cladding layer 4 to achieve both a reduction of threshold current and shortening of the lasing wavelength.

ZnMgSSe quaternary is thought to be a promising material for both reducing the threshold current and shortening the lasing wavelength. However, as mentioned above, a rapid decrease of net acceptor concentration (Na-Nd) with increasing bandgap energy in ZnMgSSe has been reported. This means that it is difficult to obtain ZnMgSSe films with a good conductivity and relatively large bandgap energy. ZnMgSSe with a relatively large bandgap energy contains relatively large amounts of S and Mg, which may result in the poor zinc blende crystal quality as the chemical composition approaches MgS because the stable crystal structure for MgS is a rocksalt structure.

To compensate for the rapid decrease of net acceptor concentration and to improve the doping efficiency, the use of modulation doping technique has been proposed by Suemune. However, in his proposal, the mechanism of carrier transport is hopping as shown in Figure 2.

The modulation doping is intended to increase the number of free holes in the valence band of the quantum wells 10 of a ZnSe/ZnSSe multiple quantum well system. In such a II-VI system, the activation energy Ea of the acceptors is very large, ranging from 110-150meV. Consequently the population of thermally activated free holes is very small. The

population of free holes in the p type ZnSe is of crucial importance since the resistivity r of the material is given by

$$r = \frac{1}{q \mu p}$$

where q = electron charge

μ = hole mobility ($\simeq$ 30 cm^2/Vs)

p = hole concentration

Therefore, in order to realise a low-resistivity and hence reduce power dissipation within the devices, an increase in the hole concentration is desirable. Suemune calculated that the free hole concentration could be increased by about 4 to 5 times for a doped superlattice having a period of 60Å. However, while the holes are free to move parallel to the quantum wells 10, transport perpendicular to the quantum wells is not so good as the holes have to hop across the quantum wells. Unfortunately it is the transport of holes perpendicular to the direction of the quantum wells which is important in the operation of many optoelectronic devices such as LEDs, lasers, detectors and modulators. There is a real possibility that the modulation doping described by Suemune could degrade the transport process along the direction perpendicular to the quantum wells since the quantum wells can act as traps for carriers (holes) which relax into them, as shown in Figure 2. The thermal activation of holes out of the quantum wells is represented by the arrows 12 and the relaxation of holes into the quantum wells is represented by the arrows 14. The relative sizes of the arrows schematically illustrate the probability of each

event with increasing probability being represented by bigger arrows. Figure 2 also indicates the energy level 6 of the first confined quantum state within each well and the energy levels 7 and 8 of the dopant materials (acceptors) within the well and barrier materials, respectively.

According to a first aspect of the present invention, there is provided a semiconductor device including a first region having a repeating pattern of first and second semiconductor regions which define a plurality of quantum wells separated from each other by quantum barriers, the pattern repeat period being sufficiently small so as to form a miniband within the first region.

The term "miniband" as used herein describes an electronic miniband which is a band of states which allow charge carriers, such as holes, to move easily.

By forming a series of closely spaced quantum wells, the quantum wave functions which extend outside of each well overlap with the wave functions of neighbouring wells. The overlapping wave functions form a miniband thereby improving carrier transport perpendicular to the quantum wells. The alternating series of semiconductor regions forms a superlattice.

The enhanced carrier transport through the valence band within the superlattice can only be achieved if the carriers can be injected into the miniband. The carriers then travel through the miniband where they may lose some energy. The main influence on whether the carriers can be transported through the miniband is the energy of the miniband relative to the energy of an injection cladding region and the energy of a

collecting cladding region. The energy minimum of the miniband within the superlattice must be greater than or equal to the potential energy level within the cladding material of a cladding layer positioned between the superlattice and an active region of the device. Similarly the energy level of an injection region must near or overlapping that of the miniband.

Preferably at least the semiconductor layers forming the quantum barriers of the superlattice are doped. This further increases the population of carriers and enhances conductivity within the first region. The quantum well regions may also be doped.

Preferably the width of the miniband is chosen to substantially maximise the transport of carriers. Preferably the carriers are holes. The width of the miniband depends upon the semiconductor materials as well as the width of the barrier and well layers, i.e. the width of the first and second semiconductor regions. Furthermore, the width of the miniband is chosen such that transport via the miniband is still possible when an electric field is placed across the first region, i.e. the miniband does not separate into Stark levels.

Preferably the semiconductors are chosen from the pseudomorphic quaternary alloys, such as Zn, Mg, S and Se. Advantageously the first and second regions form a superlattice having a ZnS_xSe_{1-x} - MgS_ySe_{1-y} ($0 \leq X, Y \leq 1$) structure.

Advantageously the widths of either of the first and second semiconductors or the repeat period of the pattern may be altered so as to vary the bandgap. The bandgap may be varied in a substantially

parabolic manner. A first superlattice may be formed to one side of an active device region and a second superlattice may be formed on an opposing side of the active device region. Each superlattice may have a spatially varying repeat period and may cooperate to define a graded index separate confinement heterostructure device. Such a structure is optically efficient.

Preferably the first and second semiconductor regions are substantially lattice matched with the lattice of a substrate such that little or no stress is exerted on the first and second semiconductor layers. The substrate may be GaAs and the lattice constants of the first and second semiconductor layers may be varied by changing the concentration of Mg and/or S within the layers.

Preferably the device is a LED, a laser, a modulator or a detector.

As an alternative, the first and second semiconductor regions may be formed of III-V semiconductor systems, such as (AlGaIn)P and (AlGaIn)N alloys.

The period repeat is preferably 6 monolayers or less. In the case of a material having a face centred cubic crystal structure, the width of a monolayer is half the lattice constant.

It is thus possible to improve carrier transport towards the active region of a device. Furthermore the superlattice can also define a graded index region to improve confinement within the active region.

The present invention will further be described, by way of example, with reference to the accompanying drawings, in which:

Figure 1 schematically illustrates an energy level diagram for a device having an active layer disposed between barrier layers;

Figure 2 schematically illustrates an energy level diagram in a modulation doping scheme as disclosed by Suemune;

Figure 3 is a schematic illustration of the bandgaps for adjacent layers of MgS and ZnSe;

Figure 4 is a schematic illustration of the energy levels for holes within a quantum well, and the broadening of the levels to form minibands;

Figure 5 is a plot of transmission probability versus energy level for a device constituting an embodiment of the present invention;

Figure 6 is a schematic illustration of the energy level versus displacement for a semiconductor device constituting an embodiment of the present invention;

Figure 7 is a plot showing bandgap and lattice constant for various semiconductors;

Figures 8a to 8c show photo-luminescence (PL) spectra for various strained layer superlattices;

Figures 9a and 9b show PL spectra for further strained layer superlattices;

Figures 10 and 11 show device structures constituting embodiments of the present invention;

Figures 12a and 12b show PL spectra for the devices illustrated in Figures 10 and 11;

Figure 13 is a graph of the I-V characteristics for the devices shown in Figure 10 and 11;

Figures 14 and 15 show devices constituting further embodiments of the present invention;

Figures 16a and 16b show PL spectra for the devices shown in Figures 14 and 15;

Figure 17 is a graph of the I-V characteristics for the devices shown in Figures 14 and 15;

Figure 18 illustrates a laser not constituting an embodiment of the present invention;

Figure 19 illustrates a laser similar to that shown in Figure 18, but constituting an embodiment of the present invention;

Figure 20 is a graph comparing output light intensity versus current for the devices shown in Figures 18 and 19;

Figures 21 to 23 illustrate further embodiments of the present invention;

Figure 24 is an energy level diagram for the device shown in Figure 23;

Figure 25 is a diagram of an energy level scheme of a laser constituting a further embodiment of the present invention; and

Figure 26 is an energy level diagram for a laser constituting another embodiment of the present invention.

As mentioned above, it is necessary to increase the bandgap energy of the cladding layer of a semiconductor laser to reduce the threshold current and to shorten the lasing wavelength. The proportions of S and Mg in ZnMgSSe can be varied to increase the bandgap thereof, but may require so much S and Mg that the structure begins to resemble MgS. This results in a poor crystal quality because the stable crystal structure for MgS is the rocksalt structure. Therefore, from the view point of crystal quality, there is an upper limit of S and Mg compositions for ZnMgSSe. However, this limit can be breached using a superlattice structure and growing MgS films with a zinc blende structure, and not a rocksalt structure. If the film thickness of MgS_ySe_{1-y} ($0 \leq y \leq 1$) is sufficiently thin, zinc blende MgS_ySe_{1-y}, can be grown on ZnS_xSe_{1-x} ($0 \leq x \leq 1$) and an upper ZnS_xSe_{1-x} layer grown over the MgS_ySe_{1-y} layer will stabilize the zinc blende structure of the MgS_ySe_{1-y} layer. The layers can be repeated to define a superlattice in which the discontinuities between the layers give a theoretical maximum band discontinuity, ΔEc (conduction band energy change) of 0 to 1115meV and ΔEv (valance band energy change) of 0 to 736meV as shown in Figure 3. Figure 3 shows two energy levels at the valence band, these levels relate to light holes (lh) and heavy holes (hh). The energy levels for the holes in an unstressed material are degenerate, however stress within the material

lifts this degeneracy. The heavy holes have a lower energy level and consequently are more populated.

Within a structure comprising first and second alternating layers, a miniband is formed as the layer thickness becomes reduced. The formation of the miniband can be considered as the superposition of a multiplicity of solutions of the "square well" otherwise known as "particle in a box" quantum mechanical problem.
To recap, the "square well" problem involves solving the Schrodinger equation,

$$\frac{-\hbar^2}{2m}\frac{d^2\Psi}{dZ^2} = E\Psi$$

for an infinitely deep well of width L_z (extending from 0 to L_z). In this solution, boundary conditions are that the wave function falls to zero at the edges of the well. Thus the solution is

$$En = \frac{\hbar^2}{2m}\left(\frac{n\pi}{L_z}\right)^2 \quad \text{where } n = 1,2,3$$

where:

m is effective mass of the particle

$\hbar$ = Planck's constant / 2π

Ψ = quantum wavefunction

and $\Psi_n = A \operatorname{Sin} \frac{n\pi Z}{L_z}$

where Z is position within the box.

However, when the height of the well becomes finite the wave functions can take non-zero values outside the confines of the well. Furthermore the solution contains both even (symmetric) solutions and odd (anti-symmetric) solutions.

The solutions to the finite well equations for a well extending from -L/2 to +L/2 give even solutions that approximate

$$\cos \frac{n\pi Z}{L}$$

within the well and antisymmetric solutions which approximate

$$\sin \frac{n\pi Z}{L}$$

within the well. Each solution also has an evanescent-wave which extends outside of the well.

The energy levels of the finite square well are similar to, but slightly lower than, the corresponding levels for the infinitely deep well solution.

Figure 4 illustrates solutions to the Schrodinger equations for the first three energy levels (n = 1 to 3) for holes within a finite well which is one of a series of wells formed by alternating layers of ZnSe and MgS. Thickness is measured in terms of monolayers of the crystal (one monolayer ≈ 2.82Å). The well and barrier thickness are substantially

identical. Starting with thicknesses of 10 monolayers, each well is effectively isolated from its neighbouring wells as the value of the evanescent wave function from neighbouring wells is substantially zero. A reduction in the number of monolayers (i.e. reducing the width of the wells and barriers) causes the energy levels of the solutions to increase - as would be expected since En is inversely proportional to the width of the well. Once the width of the wells and barriers reduces still further, the evanescent wave functions (of which the symmetric and antisymmetric solutions have different values) of the other wells begin to have significant non-zero values within the well and this splits the energy level solution into a series of values. The result of forming a series of quantum wells is that the energy levels form a continuum within a band, as indicated by the hatched regions in Figure 4.

Figure 5 illustrates the transmission probability versus energy for a heavy hole within a strained layer superlattice which has ten periods of four monolayers of ZnSe and two monolayers of MgS. The transmission probability rises as high as 0.9.

As noted above, to obtain blue light generation, it is necessary to increase the bandgap energy of cladding layer. The layer decrease of net acceptor concentration (Na-Nd) with increasing bandgap energy in ZnMgSSe makes it difficult to obtain ZnMgSSe films which have high conductivity and a large bandgap energy. Modulation doping can overcome these problems. However, in the present invention, the period of the superlattice is small enough to form a miniband, and carrier transport is carried out through the miniband (Figure 6) which results in better carrier transport than hopping (Figure 2). The period of the

superlattice should be thin enough to form a miniband, e.g. less than 6 monolayers when $d_{ZnSe} = d_{MgS}$, where d represents thickness.

Figure 6 schematically illustrates the energy level scheme within a semiconductor device constituting an embodiment of the present invention. The level scheme is similar to that shown in Figure 2 in as much as there is a plurality of quantum wells 10 defined by barriers 12. There are however two significant differences. The first is that the quantum wells and barriers are thinner (this feature is not illustrated) such that a miniband 18 can be formed. The second is that the relevant energy criteria for the holes both for injection into the miniband and for the emergence of holes from the miniband into the active region of the device are satisfied. The former condition is satisfied if the miniband energy overlaps a suitable injection energy relative to an outer cladding layer 20. The latter condition is satisfied if the minimum energy 21 of the miniband is greater than or comparable to an energy of the valence band of a further cladding material 22 positioned between the superlattice and an active region of the device. Holes are now able to propagate via the miniband 18.

The formation of a miniband at an energy comparable with the energy level of the barrier region surrounding the quantum well requires that the barriers comprising the superlattice be composed of a semiconductor material having a larger bandgap than the active region of the device. If the energy of the miniband is slightly more than the minimum energy of the cladding region, holes can still be thermally promoted into the energy band.

Figure 7 shows the bandgap energy and lattice constant for a plurality of II-VI compound semiconductors. The lattice constants of ZnSe and MgS are 5.6681Å and 5.62Å respectively, which are almost lattice matched to a GaAs substrate (5.653Å). The lattice constant of ZnSe is slightly larger than that of GaAs and the lattice constant of MgS is slightly smaller than that of GaAs. Therefore, the inner stress of a ZnSe-MgS superlattice can be made equal to zero by suitable choice of layer thickness. Stress cancellation is almost complete when $d_{ZnSe} = 2d_{MgS}$. Furthermore, by selecting the proper compositions of x and y in ZnS_xSe_{1-x}-MgS_ySe_{1-y} ($0 \leq x, y \leq 1$), the superlattice can be perfectly lattice matched to GaAs. Using a strain balanced composition, the inner stress of ZnS_xSe_{1-x}-MgS_ySe_{1-y} ($0 \leq x, y \leq 1$) superlattice can be nearly equal to zero.

Within the range of compounds ZnS_xSe_{1-x} and MgS_ySe_{1-y}, ZnSe ($x = 0$) and MgS ($y = 1$) are binary compounds, and consequently have the highest composition controllability. However, ZnS_xSe_{1-x} and MgS_ySe_{1-y}, still have a greater composition controllability than ZnMgSSe quaternary compounds.

A series of experiments have been performed to investigate the properties of devices constituting embodiments of the present invention.

To begin with, the MgS barrier thickness dependence of PL spectra of ZnSe-MgS strained layer superlattices was investigated. The strained layer superlattices were grown by molecular beam epitaxy with following growth conditions: GaAs substrate, substrate temperature of 275°C, beam equivalent pressures of Zn, Se, Mg and S are 6×10^{-7}, 1.4×10^{-6}, 1.0×10^{-7} and 2×10^{-7} Torr, respectively.

Figures 8a-c shows PL spectra at 77K for a ZnSe-MgS strained layer superlattice with a ZnSe growth time of 15 sec and with an MgS growth time of 10 sec, 20 sec and 30 sec in Figures 8a to 8c, respectively. The peak energies of the emission due to quantized energy level were (a) 3.19eV, (b) 3.31eV and (c) 3.39eV, respectively. The bandgap energy difference between all of the strained layer superlattices and ZnSe is more than 0.3eV, which means that all of the strained layer superlattices are promising as a cladding or carrier barrier layer.

In a second experiment, the ZnSe well thickness dependence of PL spectra of ZnSe-MgS strained layer superlattices was investigated. The strained layer superlattices were grown by molecular beam epitaxy with following growth conditions: GaAs substrate, substrate temperature of 275°C, beam equivalent pressures of Zn, Se, Mg and S are $8x10^{-7}$, $1.8x10^{-6}$, $1.0x10^{-7}$ and $2x10^{-7}$ Torr, respectively.

Figures 9a and 9b show PL spectra at 77K for ZnSe-MgS strained layer superlattices with MgS growth time of 10 sec and with the parameter of ZnSe growth time of 10 seconds for Figure 9a and 20 seconds for Figure 9b. The peak energies of the emission due to quantized energy level were (a) 3.20eV and (b) 2.98eV, respectively. The bandgap energy difference between strained layer superlattices with thinner ZnSe well thickness (Figure 9a) and ZnSe is more than 0.3eV, which means the strained layer superlattice with the thinner ZnSe well thickness is a more promising material as a cladding or carrier barrier layer.

In the next stage of investigation, Cl-doped strained layer superlattices were grown. The two different types of Cl-doped strained layer superlattices are shown in Figures 10 and 11.

The device shown in Figure 10 has an n-type GaAs substrate 30 which has an n-type ZnSe buffer layer 32 formed thereon. An intrinsic ZnSe-MgS strained layer superlattice 34 is formed over the buffer layer 32 and an n-type ZnSe cap layer 36 (also a buffer layer) is formed over the strained layer superlattice 34. This forms a n-i-n (Cl doped ZnSe, non-doped superlattice, Cl doped ZnSe) structure. The strained layer superlattice 34 was grown by molecular beam epitaxy with a substrate temperature of 275°C and beam equivalent pressures for Zn, Se, Mg and S of $8x10^{-7}$, $1.8x10^{-6}$, $1.0x10^{-7}$ and $2x10^{-7}$ Torr respectively and with a K-cell temperature of $ZnCl_2$ of 147°C. An indium electrode 38 is formed in contact with the substrate 1 and a further indium electrode 40 having a radius of 200μm is formed over the cap layer 36 by vacuum evaporation.

Figure 11 shows a similar device to that illustrated in Figure 10, but the intrinsic ZnSe-MgS strained layer superlattice 34 is replaced by an n-type ZnSe-MgS strained layer superlattice 42, thereby giving an n-n-n (Cl doped ZnSe, Cl doped superlattice, Cl doped ZnSe) structure.

Figures 12a and 12b show the PL spectra for the devices illustrated in Figures 9 and 10, respectively. Both devices show a peak energy of 3.21eV due to emission from a quantized energy level.

Figure 13 shows the current-voltage characteristics for the devices illustrated in Figures 10 and 11. The line labelled A refers to the device shown in Figure 10, whereas the line labelled B refers to the device shown in Figure 11. As can be seen, the n-n-n structure of Figure 11 exhibits better current flow than the intrinsic structure shown in Figure 10. This implies that the Cl-doping works effectively inside a strained layer superlattice.

Two further devices having nitrogen-doped strained layer superlattices were also fabricated. The device shown in Figure 14 has a p-type GaAs substrate 50 upon which is formed a p-type ZnSe buffer layer 52. An intrinsic type ZnSe-MgS strained layer superlattice 34 is formed over the layer 52 and a p-type ZnSe cap layer 54 is formed over the layer 34. The strained layer superlattice 34 was grown by molecular beam epitaxy with the following growth conditions: a GaAs substrate having a temperature of 275°C, beam equivalent pressures of Zn, Se, Mg and S of $8x10^{-7}$, $1.8x10^{-6}$, $1.0x10^{-7}$ and $2x10^{-7}$ Torr, respectively. This gives rise to a p-i-p (N-doped ZnSe, non-doped superlattice, N-doped ZnSe) structure. Nitrogen doping was performed by a radical doping technique with an input power of 250W and a background pressure of $4.2x10^{-7}$ Torr.

An indium electrode 38 is formed in contact with the substrate 50 and a 200μm radius gold electrode 56 is formed over the cap layer 54.

The device shown in Figure 15 is similar to that shown in Figure 14, except that the intrinsic type strained layer superlattice 34 is replaced by a p-type ZnSe-MgS strained layer superlattice 58, thereby giving rise to a p-p-p (N-doped ZnSe, N-doped superlattice, N-doped ZnSe) structure.

Figures 16a and 16b show the PL spectra at 77K for the devices shown in Figures 14 and 15, respectively. Both devices showed a peak energy level of 3.2eV due to emission from a quantized energy level.

Figure 17 shows the current versus voltage characteristics for the devices shown in Figures 14 and 15. The line labelled A relates to the device shown in Figure 14, whereas the line B relates the device shown in Figure 15. As can be seen, the device shown in Figure 15 having a p-

doped strained layer superlattice 58 has an improved current flow compared to the device shown in Figure 14. This indicates that N-doping works effectively inside the strained layer superlattice.

The above results indicate that the ZnSe-MgS strained layer superlattice is a promising cladding or carrier barrier layer.

A laser, as shown in Figure 18, was fabricated. The laser comprised an n-type GaAs substrate 30 with an n-type ZnSe cladding layer 60 formed thereon. A $Zn_{0.8}Cd_{0.2}Se$ active layer 62 is positioned above the layer 60 and a p-type ZnSe cladding layer 64 is formed above the active layer 62. Finally, a p-type contact layer 66 is formed over the p-type cladding layer 64. An indium electrode 38 makes contact with the substrate 30, whereas a 5μm wide gold electrode 68 is formed in contact with the p-type contact layer 66. The laser was cleaved from a wafer and had a cavity length of 1mm. The laser was mounted on a copper heatsink in a junction-up configuration. A second laser, illustrated in Figure 19 was also fabricated. The second laser was substantially identical to the laser illustrated in Figure 18, with the exception that a p-type ZnSe-MgS strained layer superlattice 58 was formed between the active layer 62 and the p-type ZnSe cladding layer 64.

The current versus light output characteristic for the lasers was measured at 77K in a pulsed mode having a pulse width of 2ms and a 1/5000 duty cycle. The laser mirrors were as cleaved and the strained layer superlattice 58 in the second laser (Figure 19) comprised 20 periods of four monolayer ZnSe with two monolayer MgS.

The current versus light intensity characteristic for the lasers is illustrated in Figure 20. The second laser (Figure 19) with the strained layer superlattice showed a threshold current of 10mA which was three times smaller than the equivalent laser without the strained layer superlattice. This demonstrates that the ZnSe-MgS strained layer superlattice is effective in suppressing electron overflow and encouraging better hole transport. The lasing wavelength was 490nm.

A third laser, as illustrated in Figure 21 was fabricated. The laser comprised an n-type GaAs substrate 30 having an n-type ZnSe buffer layer 32 formed thereon. An n-type $ZnS_{0.07}Se_{0.93}$ cladding layer 70 is formed over the layer 32 and has an n-type ZnSe-MgS strained layer superlattice 42 formed thereon. A ZnSe active layer 72 is formed over the strained layer superlattice 42 and has a p-type ZnSe-MgS strained layer superlattice 58 formed thereon. A p-type $ZnS_{0.07}Se_{0.93}$ cladding layer 74 is formed over the strained layer superlattice 58 and finally a p-type contact layer 66 is formed over the cladding layer 74. An indium electrode 38 makes contact with the substrate 30 and a strip electrode 68 makes contact with the contact layer 66. The laser exhibited a lasing wavelength of less than 480nm at room temperature which fell to less than 460nm at 77K. These wavelengths cannot be obtained using a ZnMgSSe quaternary compound.

A fourth laser was fabricated, as shown in Figure 22, which is similar to the laser shown in Figure 21 except that the n-type ZnSe-MgS strained layer superlattice 42 fabricated between the n-type cladding layer 70 and the active layer 72 was omitted. Lasing was observed at 77K with a wavelength of 445nm.

For the device as shown in Figures 21 and 22, the strained layer superlattice structures comprised 20 periods of 4 monolayers of ZnSe in conjunction with 2 monolayers of MgS.

A graded index separate confinement heterostructure (GRINSCH) laser was fabricated. The device structure is shown in Figure 23 and is similar to that of the device shown in Figure 21 except that the strained layer superlattices 42 and 58 at either side of the active region 72 are replaced by modulated period strained layer superlattices. The relative widths of the quantum well and quantum barrier in the modulated period strained layer superlattices are varied towards the active layers so as to provide a graded energy band profile, as schematically illustrated in Figure 24.

Figure 25 illustrates an energy level scheme for a laser having an $Mg_{0.1}ZnS_{0.14}Se$ cladding layer 90 formed over a substrate (not shown). A 500Å thick $ZnS_{0.06}Se$ barrier layer 92 is formed over the layer 90 and supports an $Cd_{0.2}ZnSe$ active layer 94 between 50 and 100Å thick. A further barrier layer 96 identical to the layer 92 covers the active layer 94. A 200Å thick $Mg_{0.1}ZnS_{0.14}Se$ cladding layer 98 provides an optical confining region between the barrier layer 96 and a superlattice 100. The superlattice consists of 10 repetitions of a 5.65Å thick layer of MgS and a 11.13Å thick layer of ZnSe. Figure 25 illustrates the relative energy levels of electrons in the condition band and holes in the valence band of such a device. Figure 25 also indicates the depth of the quantum wells formed in the superlattice as seen by electrons and holes. The chain lines 104 and 106 schematically illustrate the boundaries of the miniband and the lines 108 illustrate the acceptor energy levels of the dopant within the barrier material.

In use, electrons and holes recombine within a quantum well formed by active layer 94. The barrier layers 92 and 96 form barrier regions for the active region 94, and the layers 92 to 96 form an optical guiding region within the device. Optical radiation, and electrons and holes are confined by the cladding layers 90 and 98 and the superlattice 100. Electrons are injected into the cladding layer 90 and move towards the active layer. Electrons which pass beyond the active layer 94 are reflected by the superlattice 100 which forms an effective barrier of 172meV as indicated by the chain line 101. The holes are injected into the heavy hole miniband (defined by lines 104 and 106). The holes then travel towards the active layer 94. The transport of holes within the miniband is improved by doping at least the quantum barriers. Ea represents the activation energy of the acceptors that have been implanted into the quantum barriers by doping. Thus the superlattice 100 acts to confine electrons as well as to improve hole transport.

Figure 26 shows the energy level scheme for a laser which is similar to the device described with reference to Figure 25, except that the superlattice 100 has been replaced by a p-doped superlattice 102 having 10 repetitions of a $Mg_{0.1}ZnS_{0.14}Se$ layer 8.47Å thick and a $Mg_{0.4}ZnS_{0.4}Se$ layer 14.31Å thick. This gives less of a bandgap in the superlattice compared to the device shown in Figure 25. The operation of the device shown in Figure 26 is similar to that shown in Figure 25.

The formation of a miniband is not restricted to devices formed solely of II-VI semiconductors. Devices constituting embodiments of the present invention can also be formed from III-V semiconductor systems such as (AlGaIn)P and (AlGaIn)N alloys.

It is thus possible to provide blue light laser diodes capable of continuous operation at room temperature.

CLAIMS

1. A semiconductor device including a first region having a repeating pattern of first and second semiconductor regions which define a plurality of quantum wells separated from each other by quantum barriers, the pattern repeat period being sufficiently small so as to form a miniband within the first region.

2. A semiconductor device as claimed in Claim 1, further comprising a carrier injection region, the energy level of the injection region being substantially matched with that of the miniband.

3. A semiconductor device as claimed in Claim 1 or 2, further comprising at least one active region having an active region bandgap energy, and in which the first region acts as a barrier region for the active region and has a bandgap greater than the active region bandgap energy.

4. A semiconductor device as claimed in any one of the preceding claims, in which the first and second semiconductors consist of combinations of the pseudomorphic quaternary alloys.

5. A semiconductor device as claimed in any one of the preceding claims, in which the first semiconductor is ZnSe and the second semiconductor is MgS.

6. A semiconductor device as claimed in any one of Claims 1 to 4, in which the first semiconductor comprises ZnS_xSe_{1-x} where x is greater

than zero and less than one, and the second semiconductor comprises MgS_ySe_{1-y} where y is greater than zero and less than one.

7. A semiconductor device as claimed in any one of the preceding claims, in which at least one of the first and second semiconductors are n-type doped.

8. A semiconductor device as claimed in claim 7, in which the dopant is Cl.

9. A semiconductor device as claimed in any one of Claims 1 to 3, in which at least one of the first and second semiconductors are p-type doped.

10. A semiconductor as claimed in claim 9, in which the dopant is nitrogen.

11. A semiconductor device as claimed in any one of Claims 1 to 3, in which the first and second semiconductors are combinations of the alloy system (AlGaIn)N.

12. A semiconductor device as claimed in any one of Claims 1 to 3, in which the first and second semiconductors are combinations of the alloy system (AlGaIn)P.

13. A semiconductor device as claimed in any one of the preceding claims, in which the first and second semiconductors are lattice mismatched with respect to a substrate but combined such that they experience substantially no net strain.

14. A semiconductor device as claimed in Claim 6, in which the first and second semiconductors are lattice matched to the substrate.

15. A semiconductor device as claimed in Claim 13 or 14, in which the substrate is GaAs.

16. A semiconductor device as claimed in Claim 13 or 14, in which the substrate is ZnSe.

17. A semiconductor device as claimed in any one of the preceding claims, in which the pattern repeat period is six monolayers or less.

18. A semiconductor device as claimed in any one of the preceding claims, in which the relative thicknesses of the first and second semiconductor regions and/or the pattern repeat period vary as a function of position.

19. A semiconductor device as claimed in Claim 18, in which the first region is adjacent an active region, and in which the device further comprises a second region having a repeating pattern of third and fourth semiconductor regions, the pattern repeat being sufficiently small so as to form a miniband within the second region, and in which the active layer is sandwiched between the first and second regions.

20. A semiconductor device as claimed in Claim 19, in which the relative thicknesses of the third and fourth semiconductor regions and/or pattern repeat period vary as a function of position.

21. A semiconductor device as claimed in Claim 5, in which the first semiconductor regions are substantially twice the thickness of the second semiconductor regions.

22. A laser, comprising a semiconductor device as claimed in any one of the preceding claims.

23. A modulator, comprising a semiconductor device as claimed in any one of Claims 1 to 21.

24. A detector, comprising a semiconductor device as claimed in any one of Claims 1 to 21.

Patents Act 1977 Examiner's report to the Comptroller under Section 17 -26- (The Search report)	Application number GB 9504666.0
Relevant Technical Fields (i) UK Cl (Ed.N) H1K (KKAS) (ii) Int Cl (Ed.6) H01S H01L G02F	Search Examiner S J MORGAN Date of completion of Search 31 MAY 1995
Databases (see below) (i) UK Patent Office collections of GB, EP, WO and US patent specifications. (ii) ONLINE: WPI, INSPEC	Documents considered relevant following a search in respect of Claims :- 1-24

Categories of documents

X: Document indicating lack of novelty or of inventive step.

Y: Document indicating lack of inventive step if combined with one or more other documents of the same category.

A: Document indicating technological background and/or state of the art.

P: Document published on or after the declared priority date but before the filing date of the present application.

E: Patent document published on or after, but with priority date earlier than, the filing date of the present application.

&: Member of the same patent family; corresponding document.

Category	Identity of document and relevant passages		Relevant to claim(s)
X	EP 0614253 A1	(NEC) see whole document	1, 22, 23
X	EP 0334759 A2	(FUJITSU) see whole document	1-4, 22
X	WO 94/00884 A1	(MARTIN) see whole document	1, 2, 24
X	WO 92/08250	(MARTIN) see whole document	1, 2, 24
X	US 5324959	(HITACHI) see whole document	1, 24
X	US 4866488	(TEXAS) see whole document	1, 2, 4
X	US 4620206	(INDUSTRIAL SCIENCE) see whole document	1

Databases: The UK Patent Office database comprises classified collections of GB, EP, WO and US patent specifications as outlined periodically in the Official Journal (Patents). The on-line databases considered for search are also listed periodically in the Official Journal (Patents).